Supplementary Information

EGFR and MET receptor tyrosine kinase-altered microRNA expression induces tumorigenesis and gefitinib resistance in lung cancers.

Michela Garofalo, Giulia Romano, Gianpiero Di Leva, Gerard Nuovo, Young Jun Jeon, Apollinaire Ngankeu, Jin Sun, Francesca Lovat, Hansjuerg Alder, Gerolama Condorelli, Jeffrey A. Engelman, Mayumi Ono, Jin Kyung Rho, Luciano Cascione, Stefano Volinia, Kenneth P. Nephew, Carlo M. Croce.

Contents

Supplementary Results

Supplementary Methods

Supplementary References

Supplementary Figures 1-16

Supplementary Table 1

Supplementary Table 2

Supplementary Results.

MiR-103, 203, 30b/c and 221/222 target PKC-ε, SRC, BIM and APAF-1. Ectopic expression of miR-221/222 and miR-30b/c in H460 cells markedly decreased BIM and APAF-1 expression and enforced expression of miR-103 and -203 clearly reduced PKC-ε and SRC protein levels (**Fig. 1g,h**). Conversely, knockdown of miR-221/222 and -30b/c increased the APAF-1 and BIM protein levels (**Fig. 1i**). As MET-KD Calu-1 cells showed an increase of APAF-1 and BIM and a decrease of PKC-ε and SRC (**Fig.1j**), enforced expression of miR-221,-222 and -30b,-30c in MET-KD Calu-1 cells strongly reduced APAF-1 and BIM expression (**Supplementary Fig. 3a**), while miR-103 and -203 knockdown increased SRC and PKC-ε (**Supplementary Fig. 3b**). Collectively, these data indicate a direct correlation between change in expression of PKC-ε, SRC, APAF-1 and BIM proteins and these specific miRs after MET silencing in NSCLC cells.

MiRs deregulated after EGFR and MET knockdown. Other miRNAs commonly deregulated by EGFR/MET, including miR-21, miR-29a/c and miR-100 (**Fig.1c**), were downregulated in HCC827- and PC9-gefitinib treated cells (**Supplementary Fig. 9a**). Of note, downregulation of miR-21, -29a/c and -100 was not observed in HCC827 GR and PC9 GR after gefitinib treatment (**Supplementary Fig. 9b**); however, enforced expression of miR-21, -29a, -29c and -100 increased gefitinib resistance in HCC827 and -PC9 cells (**Supplementary Fig. 10a**). We therefore concluded that EGFR and MET control oncogenic signaling networks through common microRNAs. Recently, Seike et al. reported that miR-21 is downregulated after gefitinib treatment of NSCLC cells with EGFR activating mutations[1]. For this reason, we further investigated if miR-21 knockdown by anti-miRs oligonucleotides could restore gefitinib sensitivity in NSCLC

cells with *de novo* or acquired resistance. As expected, miR-21 knockdown increased sensitivity to gefitinib-induced apoptosis in A549, HCC827GR and PC9GR, suggesting that this miR plays a major role in the EGFR/MET signaling pathway (**Supplementary Fig. 11a,b**).

Depletion of Dicer by miR-103 reduces cell migration and promotes gefitinib sensitivity. Martello et al. recently reported that partial attenuation of Dicer by miR-103 fostered cell migration, while more complete Dicer knockdown impaired cell viability and reduced cell migration[2]. We observed a marked down-regulation of Dicer after MET silencing or miR-103 enforced expression (**Supplementary Fig. 16a**), suggesting that the almost complete silencing of Dicer by miR-103 in our system could promote the reduction of cancer cell motility and induce programmed cell death. To address this experimentally, we transfected A549 and Calu-1 cells with Dicer siRNA, inducing a significant knockdown of Dicer (**Supplementary Fig. 16b**) to levels similar to those achieved by miR-103 expression. Global attenuation of Dicer in A549 and Calu-1 cells had a significant effect on both cell migration and gefitinib resistance as compared to control cells (**Supplementary Fig. 16c,d**). Moreover, Dicer silencing reduced the expression of mesenchymal markers in Calu-1 cells and increased E-cadherin expression levels, suggesting that miR-103 induces mesenchymal-epithelial transition not only through PKC-ε but also through Dicer downregulation (**Supplementary Fig. 16e**).

Supplementary Methods

Luciferase Assay

The 3’ UTRs of human APAF-1, BIM (BCL2L11), PKC-ε and SRC genes, were PCR amplified using the following primers:

APAF-1 Fw 5’ TCT AGA CTA ATG AAA CCC TGA TAT CAA C 3’

APAF-1 Rw 5’ TCT AGA ACTGCTACCCTGAGGCACAGCCT 3’

BIM FW: 5’TCTAGACTGGATGGGACTACCTTTCTGTTC 3’

BIM RW: 5’TCTAGACATAATCCTCTGAGAATAGGCCG 3’

PKC-ε FW D 5’TCTAGAGTGACATGCAATGGCAACTCATGTGGAC 3’

PKC-ε RW D 5’ TCTAGAACAAAGAATCCCCAACACACCCCCCCAT 3’

PKC-ε FW S 5’ TCTAGATGATGCCCTGAGAGCCCACTGCAGTT 3’

PKC-ε RW S 5’ TCTAGATTGCTTCACTGCCAGGAGCCCCTGA 3’

SRC-1-21Fw 5'- GCT CTA GAG CGC AGC ACA AGG CCT TGC CTG GCC TGA TGA T -3'

SRC-1-2Rw 5'- GCT CTA GAG CCA TGG CAG TGG GTA ACA CGT CCT CTT TCA C -3'

SRC-3-4Fw 5'- GCTCTAGATCCCTGTGTGTGTGTATGTGTGTGCATGTGTGCGT 3'

SRC-3-4Rw 5'- GCT CTA GAG CGG AGA GGG ATT TGA GAG CTC GCT GGG GTG A -3'

and cloned downstream of the Renilla luciferase stop codon in pGL3 control vector (Promega). These constructs were used to generate, by inverse PCR, the p3’-UTRs-mutant-plasmids using the following primers:

APAF-1 Mut FW 5’ GTGGTTGGATGAATAATATTAATCTCCTTTTTCCC 3’

APAF-1 Mut Rw 5’ GGGAAAAAGGAGATTAATATTATTCATCCAACCAC 3’

BIM MUT FW: 5’ GTGTAAGAATGGTGCAGTGTGTTTTCCCCCTC 3’

BIM MUT RW 5’ GAGGGGGAAAACACACTGCACCATTCTTACAC 3’

PKC-ε FW MUT 1 5’ GAGA TTTTTGTATA TAGTGTTAGGCCT GTGGAATTAA TTCG 3’

PKC-ε RW MUT 1 5’ CGAATTAATTCCACAGGCCTAACACTATATACAAAAATCTC 3’

PKC-ε FW MUT 2 5’ CGTTGCATATAGAGGTATCAATGTTCAGGCATATTATAAAAC 3’

PKC-ε RW MUT 2 5’ GTTTTATAATATGCCTGAACATTGATACCTCTATATGCAACG 3’

SRC-3° Mut Fw 5’ CCAAACATGTTGTACCATGGCCCCCTCATCATAG 3’

SRC-3° Mut Rw 5’ CTATGATGAGGGGGCCATGGTACAACATGTTTGG 3’

SRC-4° mut Fw 5’ GGCCAAGCAGTGCCTGCCTATGAACTTTTCCTTTCATACG 3’

SRC-4° mut RW 5’CGTATGAAAGGAAAAGTTCATAGGCAGGCACTGCTTGGCC 3’

MeG01 cells were cotransfected with 1µg of p3’UTR-APAF-1, p3’UTR-BIM, p3’UTR-PKC-ε p3’UTR-SRC and with p3’UTRmut-APAF-1, p3’UTR-mut-BIM, p3’UTR-mut-PKC-ε, p3’UTR-mut-SRC plasmids and 1 µg of a Renilla luciferase expression construct pRL-TK (Promega) by using Lipofectamine 2000 (Invitrogen). Cells were harvested 24h post-transfection and assayed with Dual Luciferase Assay (Promega) according to the manufacturer’s instructions. Three independent experiments were performed in triplicate.

Western Blot Analysis.

Total proteins from NSCLC were extracted with radioimmunoprecipitation assay (RIPA) buffer (0.15mM NaCl, 0.05mM Tris-HCl, pH 7.5, 1% Triton, 0.1% SDS, 0.1% sodium deoxycholate and 1% Nonidet P40). Sample extract (50 µg) was resolved on 7.5–12% SDS–polyacrylamide gels (PAGE) using a mini-gel apparatus (Bio-Rad Laboratories) and transferred to Hybond-C extra nitrocellulose. Membranes were blocked for 1h with 5% nonfat dry milk in Tris-buffered saline containing 0.05% Tween 20, incubated overnight with primary antibody, washed and incubated with secondary antibody, and visualized by chemiluminescence. The following primary antibodies

were used: Apaf-1, Snail, Slug (abcam), Src, Met, Dicer, Vimentin, E-cadherin, Zeb1, Zeb-2 (Santa Cruz), Bim, p-Erks, total Erks, pAkt, total Akt, GAPDH, Parp (cell signaling), Pkc-ε (BD transduction lab), β-actin antibody, Fibronectin (Sigma). A secondary anti-rabbit or anti-mouse immunoglobulin G (IgG) antibody peroxidase conjugate (Chemicon) was used.

Real-time PCR

Real-time PCR was performed using a standard TaqMan PCR Kit protocol on an Applied Biosystems 7900HT Sequence Detection System (Applied Biosystems). The 10 µl PCR reaction included 0.67 µl RT product, 1 µl TaqMan Universal PCR Master Mix (Applied Biosystems), 0.2 mM TaqMan probe, 1.5 mM forward primer and 0.7 mM reverse primer. The reactions were incubated in a 96-well plate at 95 ˚C for 10 min, followed by 40 cycles of 95 ˚C for 15 s and 60 ˚C for 1 min. All reactions were run in triplicate. The threshold cycle (CT) is defined as the fractional cycle number at which the fluorescence passes the fixed threshold. The comparative CT method for relative quantization of gene expression (Applied Biosystems) was used to determine miRNA and genes expression levels. The y axis represents the $2^{(-\Delta CT)}$, or the relative expression of the different miRs and genes. MiRs expression was calculated relative to U44 and U48 rRNA (for microRNAs) and to GAPDH (for genes). Experiments were carried out in triplicate for each data point, and data analysis was performed by using software (Bio-Rad).

shRNA Lentiviral Particles Transduction. Cells were plated in a 12-well plate 24 hours prior to viral infection and incubated overnight with 1ml of complete optimal medium (with serum and antibiotics). The day after the medium was removed and 1 ml of complete medium with Polybrene (5µg/ml) was added. The day after, cells were infected by adding 50 µl of control shRNA, shEGFR, shMET Lentiviral Particles (Santa Cruz) to the cultures. Stable clones were selected via 1µg/ml of Puromycin dihydrochloride.

RNA extraction and Northern blotting

Total RNA was extracted with TRIzol solution (Invitrogen), according to the manifacturer's instructions and the integrity of RNA was assessed with an Agilent BioAnalizer 2100 (Agilent, Palo Alto, CA, USA). Northern blotting was performed as described by Calin et al.[3] The oligonucleotides used as probes were the complementary sequences of the mature miRNA (miRNA registry):

miR-103: 5'TCATAGCCCTGTACAATGCTGCT3';

miR-203: 5'CTAGTGGTCCTAAACATTTCAC3';

miR-30b: 5' AGCTGAGTGTAGGATGTTTACA

miR-30c: 5'GCTGAGAGTGTAGGATGTTTACA3';

miR-221: 5'GAAACCCAGCAGACAATGTAGCT3';

miR-221: 5' ACCCAGTAGCCAGATGTAGTAGCT 3'

PKCε, SRC, BIM, APAF-1 siRNAs transfection.

Cells were cultured to 50% confluence and transiently transfected using Lipofectamine 2000 with 100 nM anti-PKC-ε, anti-SRC, anti-BIM anti-APAF-1 or control siRNAs (Santa Cruz), a pool of three target specific 20–25 nt siRNAs designed to knock down gene expression.

MiRNA locked nucleic acid in situ hybridization of formalin fixed, paraffin-embedded tissue section.

In situ hybridization (ISH) was carried out on deparaffinized human lung tissues using previously published protocol[4], which includes a digestion in pepsin (1.3 mg/ml) for 30 minutes. The sequences of the probes containing the dispersed locked nucleic acid (LNA) modified bases with digoxigenin conjugated to the 5' end were: miR-222 (5') ACCCAGTAGCCAGATGTAGCT; miR-103-(5') AGCAGCATTGTACAGGGCTATGA (3'); miR-203-(5') CTAGTGGTCCTAAACATTTCAC 3'; miR-30c-(5') GCTGAGAGTGTAGGATGTTTACA 3'. The probe cocktail and tissue miRNA were co-denatured at 60˚C for 5 minutes, followed by hybridization at 37 ˚C overnight and a stringency wash in 0.2X SSC and 2% bovine serum albumin at 4˚C for 10 minutes. The probe-target complex was seen due to the action of alkaline phosphatase on the chromogen nitroblue tetrazolium and bromochloroindolyl phosphate (NBT/BCIP). Negative controls included the use of a probe which should yield a negative result in such tissues (scrambled miRNA). No counterstain was used, to facilitate co-labeling for PKC-ε, APAF-1, SRC, BIM and MET proteins. After in situ hybridization for the miRNAs, as previously described (Nuovo et al., 2009), the slides were analyzed for immunohistochemistry (IHC) using the optimal conditions for SRC (1:100, cell conditioning for 30 minutes), PKC-ε (1:10, protease digestion for 4 minutes) BIM (1:100, cell conditioning for 30 minutes), APAF-1 (1:25, cell conditioning for 30 minutes) and MET (1:50, cell

conditioning for 30 minutes). The 30 indipendent tumor specimens were analyzed by IHC using the optimal condition for MET (1:50, cell conditioning for 30 minutes) and EGFR (1:100, cell conditioning for 30 minutes). For the immunohistochemistry, we used the Ultrasensitive Universal Fast Red or DAB systems from Ventana Medical Systems. The percentage of tumor cells expressing PKC-ε, SRC, BIM, APAF-1, MET and miR-103, miR-203, miR-30c, miR-221/222 was then analyzed with emphasis on co-localization of the respective targets. Co-expression analysis was done with the Nuance system (Cambridge Research Institute) per the manufacturer's recommendations.

Lung cancer samples and cell lines.

110 cancer lung tissues were purchased from US Biomax, Inc. 40 lung tumor tissue samples were provided from the Department of Pathology, Ohio State University. All human tissues were obtained according to a protocol approved by the Ohio State Institutional Review Board. Human Calu-1 cell lines were grown in Dulbecco's modified Eagle's medium containing 10% heat-inactivated fetal bovine serum (FBS) and with 2mM L-glutamine and $100Uml^{-1}$ penicillin–streptomycin. A549, H460, H1299, H1573, H292, HCC827, PC9, HCC827 GR, PC9GR cell lines were grown in RPMI containing 10% heat-inactivated FBS and with 2mM L-glutamine and $100Uml^{-1}$ penicillin–streptomycin.

Bioinformatics analysis

Bioinformatics analysis was performed by using these specific programs: Targetscan[1], Pictar[2], RNhybrid [3].

[1]http://www.targetscan.org/

[2] http://pictar.bio.nyu.edu/

[3] http://bibiserv.techfak.uni-bielefeld.de/

Generation of Stable Clones with miR-103 and miR-203 overexpression and miR-221, -30c downregulation.

A549 cells were stably infected with the Human pre-microRNA Expression Construct Lenti-miR expression plasmid containing the full-length miR-103, miR-203 or the anti-miR-221, -30c and the GFP gene under the control of two different promoters (System Biosciences). An empty vector was used as control. Pre-miRs expression and control constructs were packaged with pPACKH1 Lentivector Packaging Plasmid mix (System Biosciences) in a 293TN packaging cell line. Viruses were concentrated using PEGit Virus Precipitation Solution, and titers were analyzed using the UltraRapid Lentiviral Titer Kit (System Biosciences). Infected cells were selected by FACS analysis (FACScalibur; BD Bioscience). Infection efficiency >90% was verified by fluorescent microscopy and confirmed by real-time PCR for miRs expression.

Generation of miR-30b/c- and 221/222- insensitive BIM and APAF-1 cDNAs.

Bim and APAF-1 WT and mutated 3'UTRs were amplified and cloned downstream of the APAF-1 and BIM coding sequences (Origene) by using the following primers:

APAF-1 FW 5' GGCCGGCC CTA ATG AAA CCC TGA TAT CAA C 3'

APAF-1 RW 5' GGCCGGCC ACTGCTACCCTGAGGCACAGCCT 3'

BIM FW: 5'GGCCGGCCCTGGATGGGACTACCTTTCTGTTC 3'

BIM RW: 5'GGCCGGCCCATAATCCTCTGAGAATAGGCCG 3'

The constructs were then used to perform viability and caspase 3/7 assays. Experiments were performed at least three times in triplicate.

Scratch Assay

A549 cells were transfected with control miR, miR-103 or miR-203 for 72h. 24h after transfection cells were incubated with medium 5% FBS. Images were acquired directly after scratching (0h) and after 24h. Quantization of migration distance using Image J software. The distance covered was calculated by converting pixel to millimeters.

Cell-Cycle Analysis

For cell-cycle analysis, cells were plated in 6 cm dishes, transfected as indicated in the figures, trypsinized, washed in PBS, and fixed with ice-cold 70% ethanol while vortexing. Cells were rehydrated in PBS and stained 30 min at RT with propidium iodide (50 mg/ml PI, 0.5 mg/ml RNase in PBS) prior to flow-cytometric analysis. Every experiment was repeated 5 times independently, with two replicas for each sample.

Supplementary References

1. 1. Seike, M., *et al.* MiR-21 is an EGFR-regulated anti-apoptotic factor in lung cancer in never-smokers. *Proc Natl Acad Sci USA* **106**, 12085-90 (2009).

2. Martello, G., *et al.* A MicroRNA targeting dicer for metastasis control. *Cell.* **141,** 1195-207 (2010).

3. Calin, G.A., *et al*. Frequent deletions and down-regulation of micro-RNA genes miR15 and miR16 at 13q14 in chronic lymphocytic leukemia. *Proc Natl Acad Sci U S A.* **99**, 15524-9 (2002).

4. Nuovo, G.J., *et al*. A methodology for the combined *in situ* analyses of the precursor and mature forms of microRNAs and correlation with their putative targets. *Nature Protocols* **4**, 107-115 (2009).

a

Table 1 Calu-1-shEGFR

microRNA	Fold change	p value
hsa-miR-361-5p	-10.7	1.3E-03
hsa-miR-301	-8.58	1.9E-03
hsa-miR-324	-6.37	2.1E-03
hsa-miR-636	-4.36	9.3E-03
hsa-miR-30c	-2.4	1.2E-03
hsa-miR-99b	-2.3	4.06E-02
hsa-miR-15b	-2.31	1.2E-02
hsa-miR-197	-2.16	5.2E-03
hsa-miR-125b	-2.10	4.7E-02
hsa-miR-193a-3p	-1.87	9.25E-03
hsa-miR-30b	-1.81	3.5E-02
hsa-miR-221	-1.79	1.1E-03
hsa-miR-182	-1.75	1.4E-02
hsa-miR-130b	-1.69	1.6E-02
hsa-miR-222	-1.66	5.2E-03
hsa-miR-99a	-1.64	1.7E-03
hsa-miR-21	-1.56	5.4E-02
hsa-miR-100	-1.55	6.1E-03
hsa-miR-210	-1.54	1.64E-02
hsa-miR-125a	-1.53	2.07E-02
hsa-miR-29c	-1.53	3.0E-04
hsa-miR-29a	-1.52	3.2E-02
hsa-miR-200a	-1.51	3.8E-02
miR-101	4.0	1.0E-02

Table 2 Calu-1-shMET

microRNA	Fold change	p value
hsa-miR-548d-5p	-14.46	3.81E-02
hsa-miR-652	-3.6	1.52E-03
hsa-miR-30c	-4.0	1.46E-02
hsa-miR-135b	-2.37	3.53E-03
hsa-miR-30b	-3.5	3.11E-02
let-7a	-2.13	3.64E-02
hsa-miR-221	-2.07	3.45E-03
hsa-miR-29c	-1.79	2.8E-03
let-7e	-1.78	4.14E-02
hsa-miR-26b	-1.76	1.36E-02
hsa-miR-222	-1.75	8.35E-03
miR-146a	-1.74	3.21E-03
hsa-miR-200b	-1.72	9.27E-03
hsa-miR-29a	-1.72	2.91E-02
hsa-miR-20a	-1.72	2.6E-03
hsa-miR-100	-1.72	3.16E-02
hsa-miR-365	-1.7	1.33E-02
hsa-miR-21	-1.7	2.13E-02
hsa-miR-29b	-1.7	9.30E-03
hsa-miR-203	2.5	9.2E-03
hsa-miR-103	2.45	8.23E-03
hsa-miR-200c	2.3	3.33E-02
hsa-miR-328	2.29	9.11E-04
hsa-miR-218	1.88	4.3E-03

b

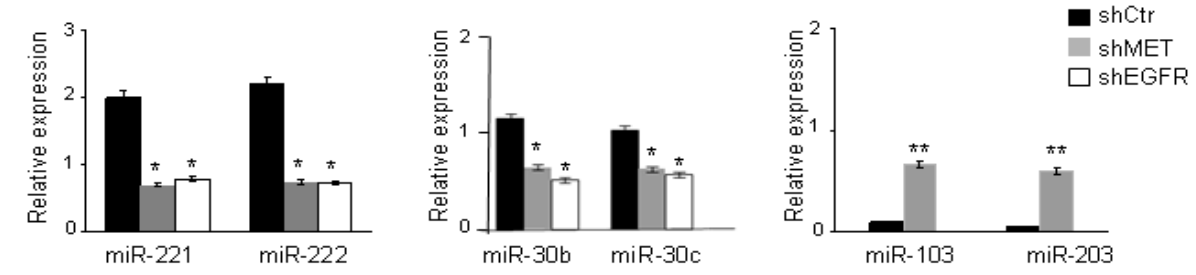

Supplementary Figure 1. MicroRNAs deregulated after stable EGFR and MET silencing. (a) MicroRNAs deregulated after EGFR (Table 1) and MET (Table 2) silencing, with >1.5- (EGFR) and with >1.7 (MET) -fold changes are shown ($P<0.05$). Green = downregulated miRs; Red = upregulated miRs. **(b)** qRT-PCR showing miR-221/222 and -30b/c downregulation after MET and EGFR silencing and miR-103 and -203 upregulation after MET silencing. Data are means ± s.d. of three independent experiments. *$P<0.001$, **$P<0.0001$.

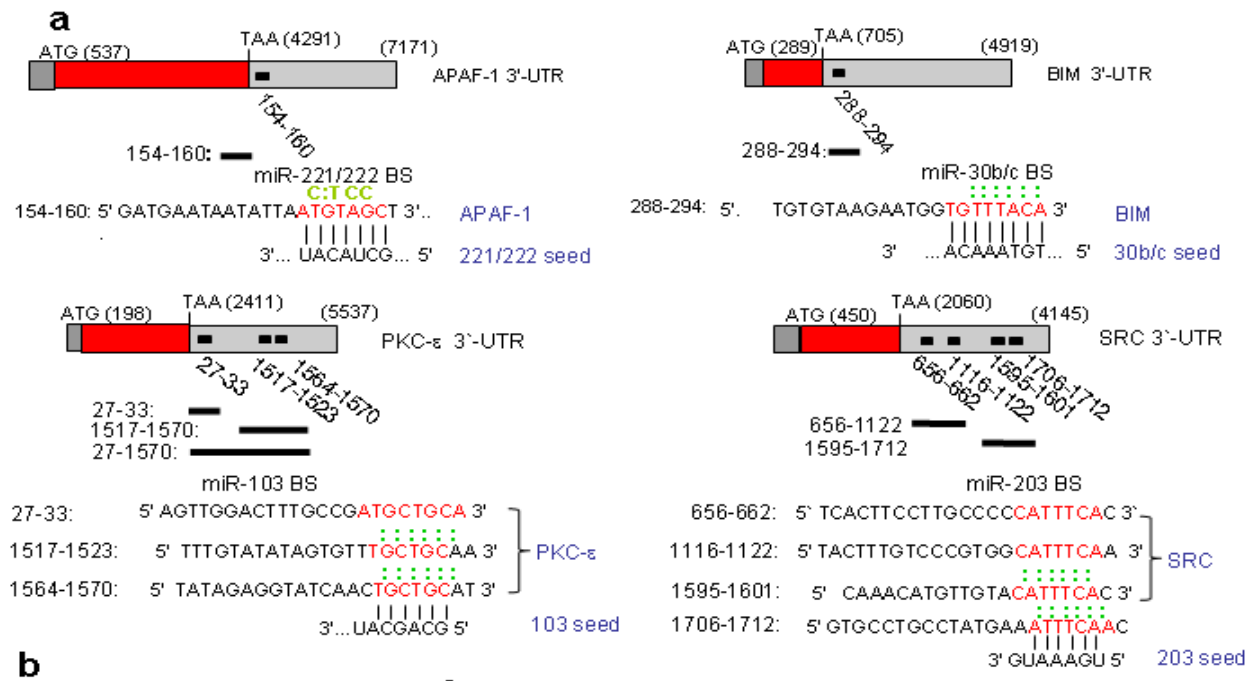

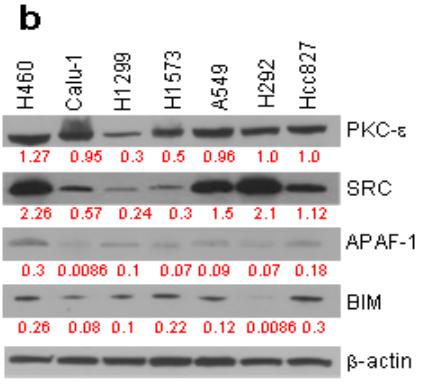

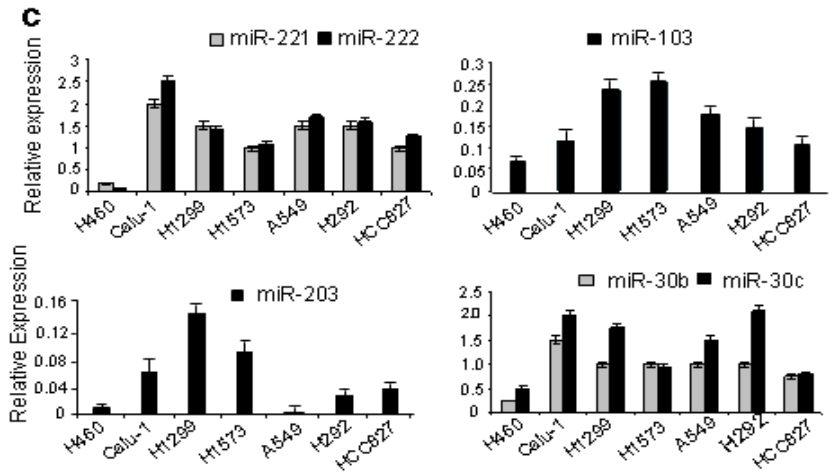

d

Pearson correlation	SRC	miR-203	PKC-ε	miR-103	BIM	miR-30c	APAF-1	miR-222
SRC	1	-.892*	.180	-.690	-.158	.205	-.146	.220
N	7	7	7	7	7	7	7	7
miR-203	-.892*	1	.096	.641	.192	-.217	.162	-.315
N	7	7	7	7	7	7	7	7
PCK-ε	.180	.096	1	-420*	-163	.272	-120	.320
N	7	7	7	7	7	7	7	7
miR-103	-590	.641	-.420*	1	.042	-.322	0.102	-.132
N	7	7	7	7	7	7	7	7
BIM	-.158	.192	-.163	.042	1	-.883	.212	-.125
N	7	7	7	7	7	7	7	7
miR-30c	-.204	.417	.272	.322	-.883*	1	-.222	.371
N	7	7	7	7	7	7	7	7
APAF-1	-.146	.162	-120	102	.212	-222	1	-423*
N	7	7	7	7	7	7	7	7
miR-222	.220	-.315	.320	-132	-.125	.371	-423*	1
N	7	7	7	7	7	7	7	7

*Correlation is significant at the 0.01 level (2-tailed)

Supplementary Figure 2. MiR-221/222, 30b-c, 103 and 203 predicted targets. (**a**) APAF-1 3'UTR presents one miR-221/222 binding site (nucleotides 154-160); BIM presents one miR-30b/c binding site (nt 288-294); PKC-ε presents three miR-103 binding sites (nt 27-33, 1517-1523, 1564-1570); SRC 3'UTR presents four miR-203 binding sites (nt 656-662, 1116-1122, 1595-1601, 1706-1712). In the figure the alignment of the seed regions of miR-221&222 with APAF-1, miR-30b/c with BIM, miR-103 with PKC-ε and miR-203 with SRC 3'UTRs is shown. The sites of target mutagenesis are indicated in green. **:** = deleted nucleotides. 370 and 342 bp of the 3' UTRs for APAF-1 and BIM were amplified, respectively. Three different constructs for PKC-ε (27-33 (bp=385), 1517-1570 (bp=496), 27-1570 (bp=1720)) and two for SRC (656-1122 (bp=705), 1595-1712 (bp=805)) were generated. BS= binding site. (**b**) Western blots in a panel of 7 NSCLC cells. Protein abundance is reported as western blotting densitometry normalized to β-actin expression. (**c**) qRT-PCR showing low expression of miR-103, -203, as compared with miR-221/222, -30b/c relative expression levels, in a panel of NSCLC cells. (**d**) The association between miR-103,-203,-30b/c, -221/222 and *PKC-ε, SRC*, *BIM* and *APAF-1* mRNAs in the 7 NSCLC cells was calculated statistically by using the Pearson Correlation Coefficient (r) and the respective *p*-values, all significant at $P<0.01$. The Pearson correlation indicated an inverse relation between miR-103, -203, -30c, -222 and *PKC-ε, SRC*, *BIM* and *APAF-1* mRNAs in all the cells analyzed. Results are representative of at least, three independent experiments. Error bars depict ± s.d.

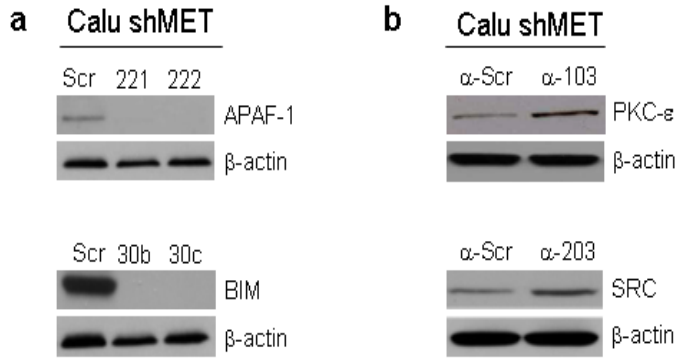

Supplementary Figure 3. MiR-221/222, 30b/c, 103, 203 target APAF-1, BIM, PKC-ε and SRC. (**a**) Calu-1 MET–KD cells, transfected with miR-221/222 and -30b/c, present a decrease in APAF-1 and BIM protein levels; (**b**) conversely, anti-miR-103 and -203 increase PKC-ε and SRC expression, respectively. Scr= scrambled. Results are representative of at least, three independent experiments.

a

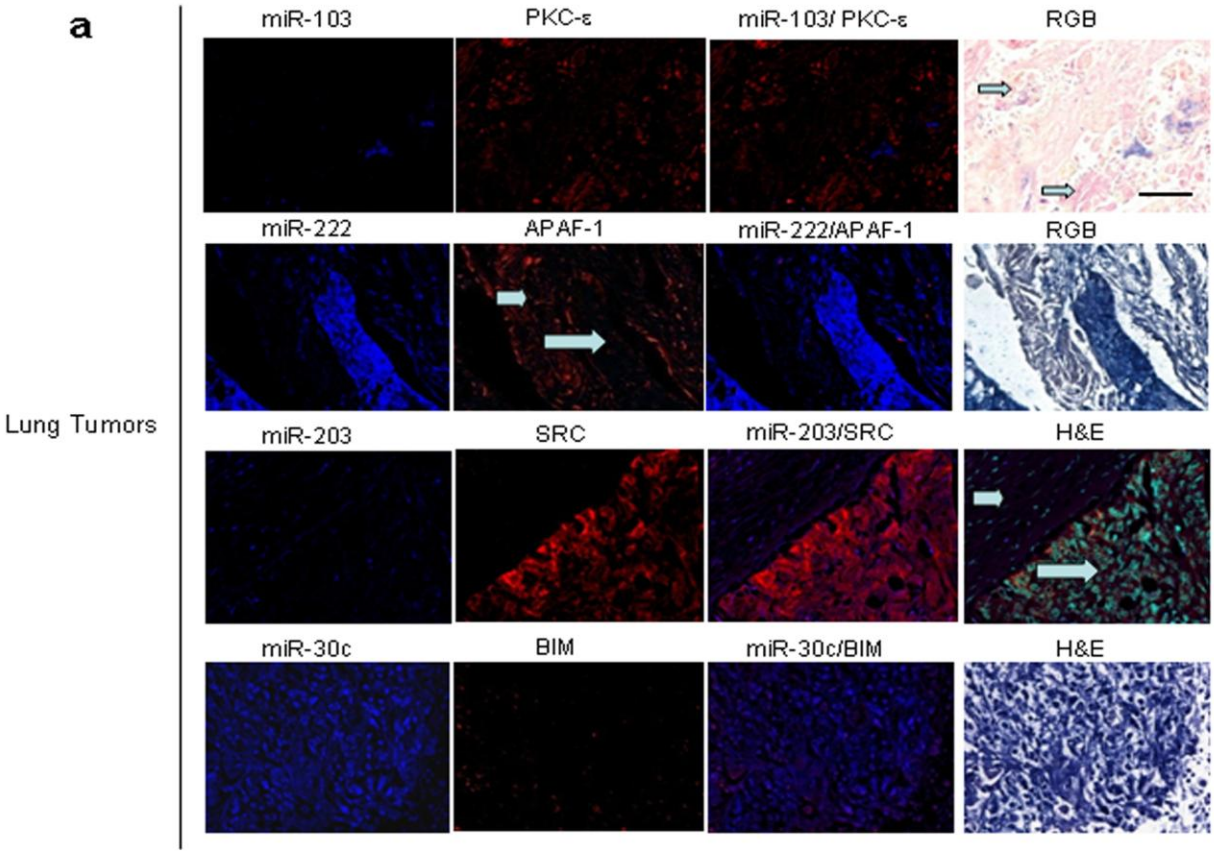

b

Table 1

	PKCε+	PKCε -
miR-103 +	2%	7%
miR-103 -	44%	47%

Table 2

	APAF-1 +	APAF-1 -
miR-222 +	20%	43%
miR-222 -	17%	20%

Table 3

	SRC+	SRC -
miR-203 +	1%	27%
miR-203 -	40%	32%

Table 4

	BIM+	BIM -
miR-30c +	1%	46%
miR-30c -	24%	29%

Supplementary Figure 4. MiR-103-PKC-ε, 222-APAF-1, 203-SRC and 30c-BIM co-expression analyses. (**a**) 110 lung cancer tissues were analyzed for miR-103, -222,-203,-30c expression by ISH and then for PKC-ε, APAF-1, SRC and BIM by IHC. Upper row, from the left miR-103 (blue) and PKC-ε (red) results show a weak signal for the miRNA and a strong signal for the protein in this lung cancer. Mixing of the images (third panel) shows no co-expression of the two targets, which would appear as yellow; note the localization of the PKC-ε signal (red) to the nests of cancer cells (arrows). Second row, left panel is a strong miR-222 signal and a weak signal for the putative target APAF-1 in the cancer cells (large arrow, second panel), but not the surrounding benign stromal cells (small arrow). Third panel shows no detectable co-expression. Third row, left panel is miR-203 (blue), next is the SRC signal (red) and the mixed signal; note the lack of miR-203 and SRC co-expression. In the right panel the counterstain hematoxylin is added as fluorescent turquoise. This allows one to see that the cancer cells (large arrow) are expressing SRC and not the benign desmoplastic cells (small arrow). Last row, left panel is miR-30c signal (blue), next BIM (red) and the merged image where the lack of yellow indicates no co-expression of the two targets. Right panels show the regular color-based image (RGB = Red, Green, Blue). Scale bar indicates 100 μm. (**b**) Tables showing the inverse relation between microRNAs and protein targets expression in 110 lung tumors.

a

	Low expression of c-Met* (48%)	High expression of c-Met* (52%)
miR-30c	45%	55%
miR-103	81%	19%
miR-203	64%	36%
miR-222	39%	61%

*Low expression was defined by <30% of the tumor cells. High expression was defined by 30% or higher of the tumor cells.

b

	Lung cancers with metastases	Lung cancers with no metastases
MET +	36	21
MET -	21	32

c

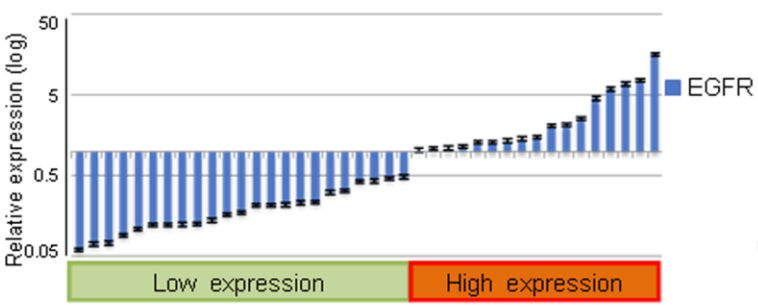

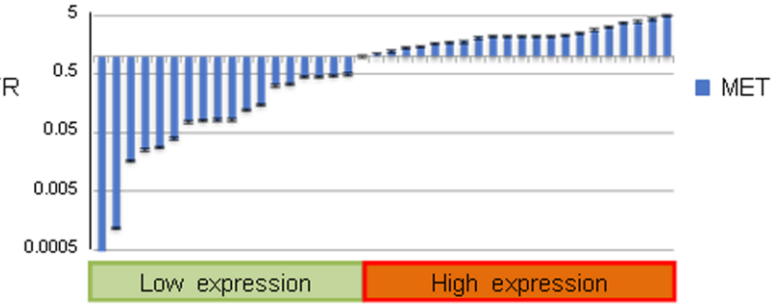

d

qRT-PCR	IHC +	IHC -
High	22	0
Low	0	18

MET

qRT-PCR	IHC +	IHC -
High	16	1
Low	0	23

EGFR

e

	Lung cancers with metastases	Lung cancers with no metastases
MET +	13	9
MET -	4	14

	Lung cancers with metastases	Lung cancers with no metastases
EGFR +	5	12
EGFR -	12	11

Supplementary Figure 5. MET is overexpressed in metastatic lung tumor tissues. (**a**) Table reporting the percentage of MET and miR-30c, -103, -203, 222 expression observed in the 110 tumor samples analyzed. MiR-103 and -203 are inversely correlated and miR-30c and -222 directly correlated to MET expression in the majority of the tumor specimens. (**b**) Percentage of metastatic and non-metastatic lung tumor samples expressing MET. MET is overexpressed in the metastatic tumors compared to the lung non-metastatic tissues. P = 0.021 by Fisher's exact test. (**c**) 40 lung tumors were divided in "high" and "low" EGFR and MET expression by qRT-PCR by round function with the cutoff at 0.5 **(**$2^{(-\text{DeltaCt})}$ **).** (**d**) 2×2 contingency table showing the association between IHC analysis and qRT-PCR results for EGFR and MET. $P < 0.0001$ by Fisher exact test. (**e**) Tables showing the number of metastatic tumors expressing MET and EGFR in the 40 lung cancers. Note the direct relation between metastases and MET but not EGFR expression levels. MET, P =0.026; EGFR, P = not significant by Fisher's exact test.

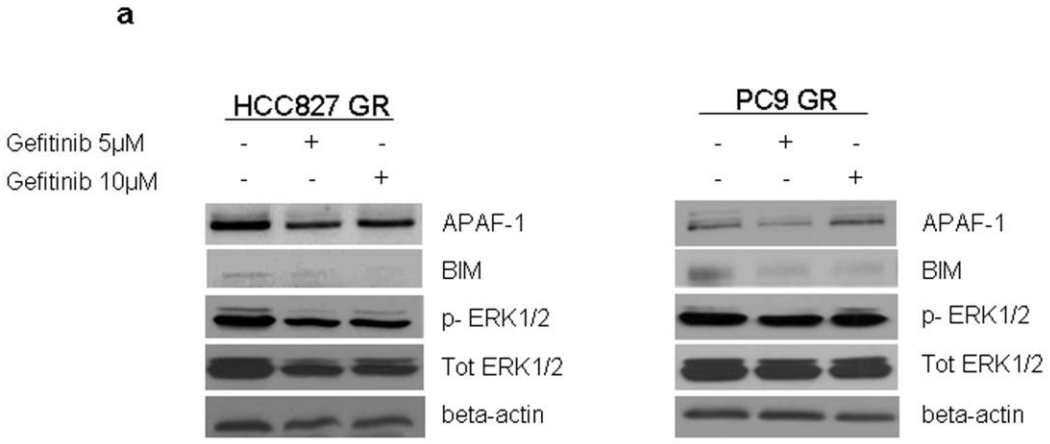

Supplementary Figure 6. APAF-1 and BIM expression in PC9GR and HCC827GR cells. (**a**) HCC827GR and PC9GR cells were treated with 5 or 10 μM gefitinib for 24h. APAF-1 and BIM expression and ERKs phosphorylation did not change after gefitinib treatment, as a consequence of miR-221/222 and -30b/c unchanged expression. β-actin was used as loading control.

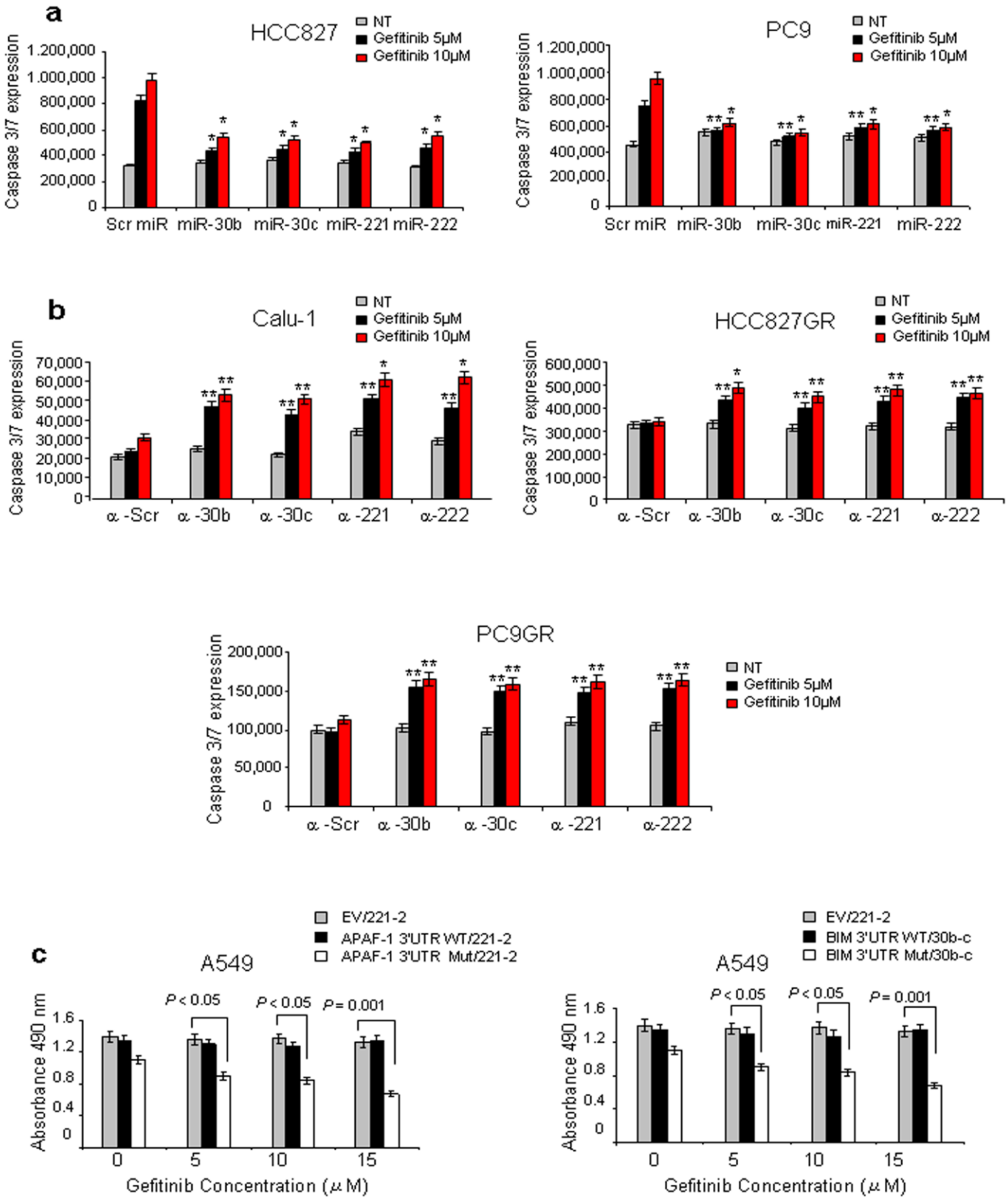
a
HCC827
NT
Gefitinib 5μM
Gefitinib 10μM
Caspase 3/7 expression
1.200,000
1.000,000
800,000
600,000
400,000
200,000
0
Scr miR
miR-30b
miR-30c
miR-221
miR-222
PC9
b
Calu-1
70,000
60,000
50,000
40,000
30,000
20,000
10,000
α -Scr
α -30b
α -30c
α -221
α-222
HCC827GR
600,000
500,000
400,000
300,000
200,000
100,000
PC9GR
200,000
150,000
100,000
50,000
c
EV/221-2
APAF-1 3'UTR WT/221-2
APAF-1 3'UTR Mut/221-2
A549
P < 0.05
P < 0.05
P = 0.001
Absorbance 490 nm
1.6
1.2
0.8
0.4
Gefitinib Concentration (μM)
BIM 3'UTR WT/30b-c
BIM 3'UTR Mut/30b-c

Supplementary Figure 7. MiR-30b, 30c, 221, 222 are involved in gefitinib-induced apoptosis. (**a**) Enforced expression of miR-30b,-30c, -221, -222 increases resistance to gefitinib induced apoptosis in HCC827 and PC9 sensitive cells as assessed by caspase 3/7 assay. (**b**) MiR-30b, -30c, -221, -222 knockdown increases gefitinib sensitivity in NSCLC cells with *de novo* (Calu-1) and acquired (HCC827GR and PC9GR) resistance to TKIs. (**c**) A549 were cotransfected with miR-30b/c, -221/222 and APAF-1 and BIM cDNAs followed by their 3'UTRs, containing the WT or mutated miRNA binding sites. Overexpression of miR-30b/c- and 221/222- insensitive BIM and APAF-1 cDNAs, induces gefitinib sensitivity in A549 cells by MTS assay**.** All experiments were performed at least three times with essentially identical results. One representative of three independent experiments is shown. Two tailed student's t test was used to determine *P* values. Error bars depict $\pm$ s.d. **P*<0.001, ***P*<0.05.

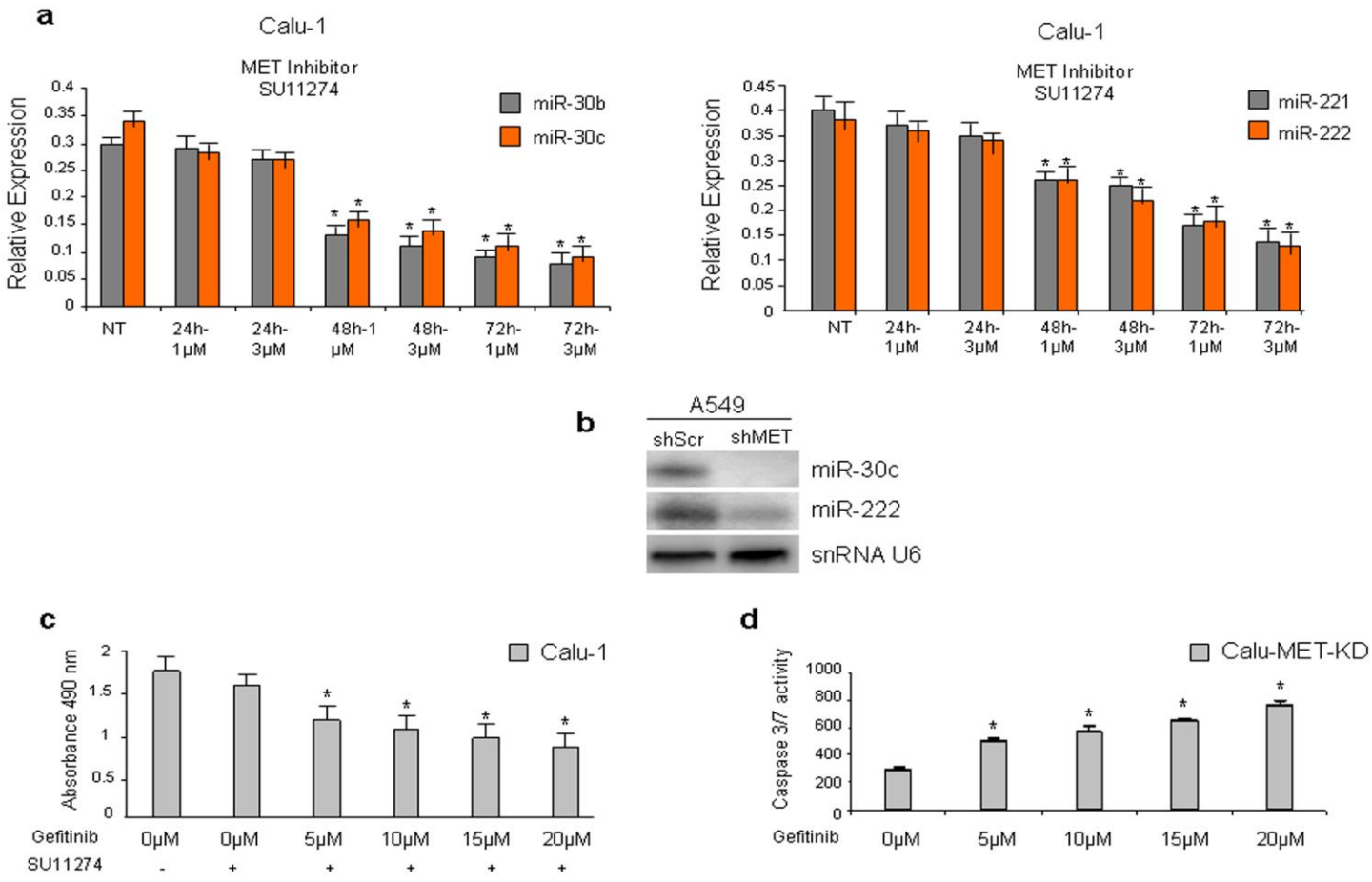

Supplementary Figure 8. MET inhibition induces down-regulation of miR-30b-c and 221-222. (**a**) qRT-PCR showing miR-30b/c and miR-221/222 down-regulation after treatment of Calu-1 cells with SU11274. Cells were treated with the MET inhibitor for 24, 48 and 72h at a concentration of 1 and 3 μM. RNA extraction and qRT-PCR were performed as described in the Supplementary methods. Results from three different experiments are shown. (**b**) Northern blots showing miR-30c and miR-222 down-regulation in A549 cells after MET KD. SnRNA U6 was used as loading control. (**c**) Calu-1 cells were treated with the MET inhibitor SU11274. After 24h cells were exposed to gefitinib (5-10-15-20 μM) for 24h. MET inhibition increased Calu-1 sensitivity to the drug as assessed by

MTS assay (**d**) Calu-1-MET knockdown cells (Calu-MET-KD) treated with gefitinib (5-10-15-20 μM) for 24h were more sensitive to gefitinib as assessed by caspase 3/7 assay. Experiments were performed three times in triplicate. Error bars represent standard deviation. Two-tailed *t* test was used to determine all *P* values. **P*<0.001.

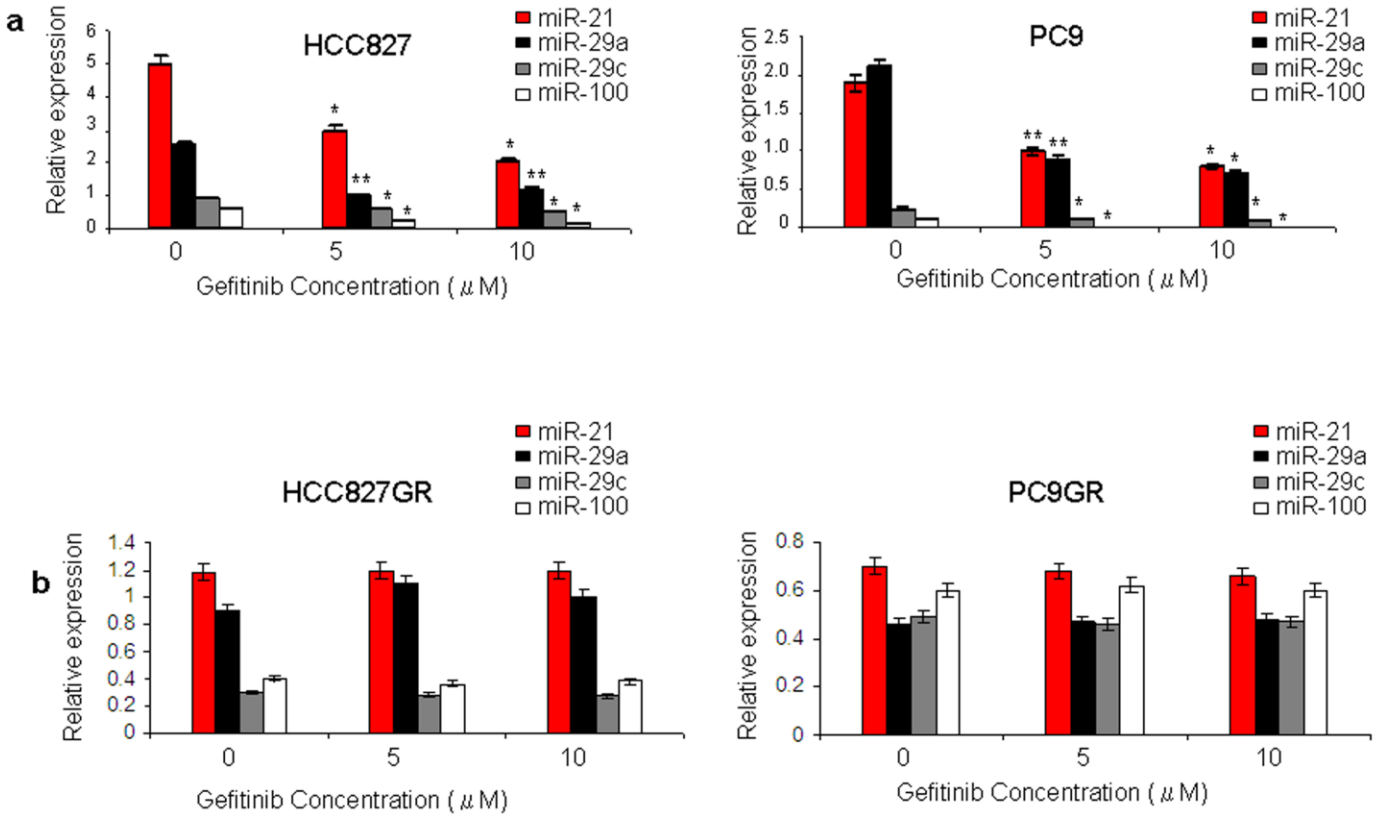

Supplementary Figure 9. EGFR and MET regulated miRNAs involved in gefitinib resistance. (**a-b**) qRT-PCR showing miR-21, -29a, -29c and -100 downregulation in HCC827 and PC9 but not in HCC827GR and PC9GR cells after treatment with 5 and 10

μM gefitinib**.** Relative values are shown as mean and ± s.d. Two tailed student's t test was used to determine *P* values.* P<0.005, **P<0.001.

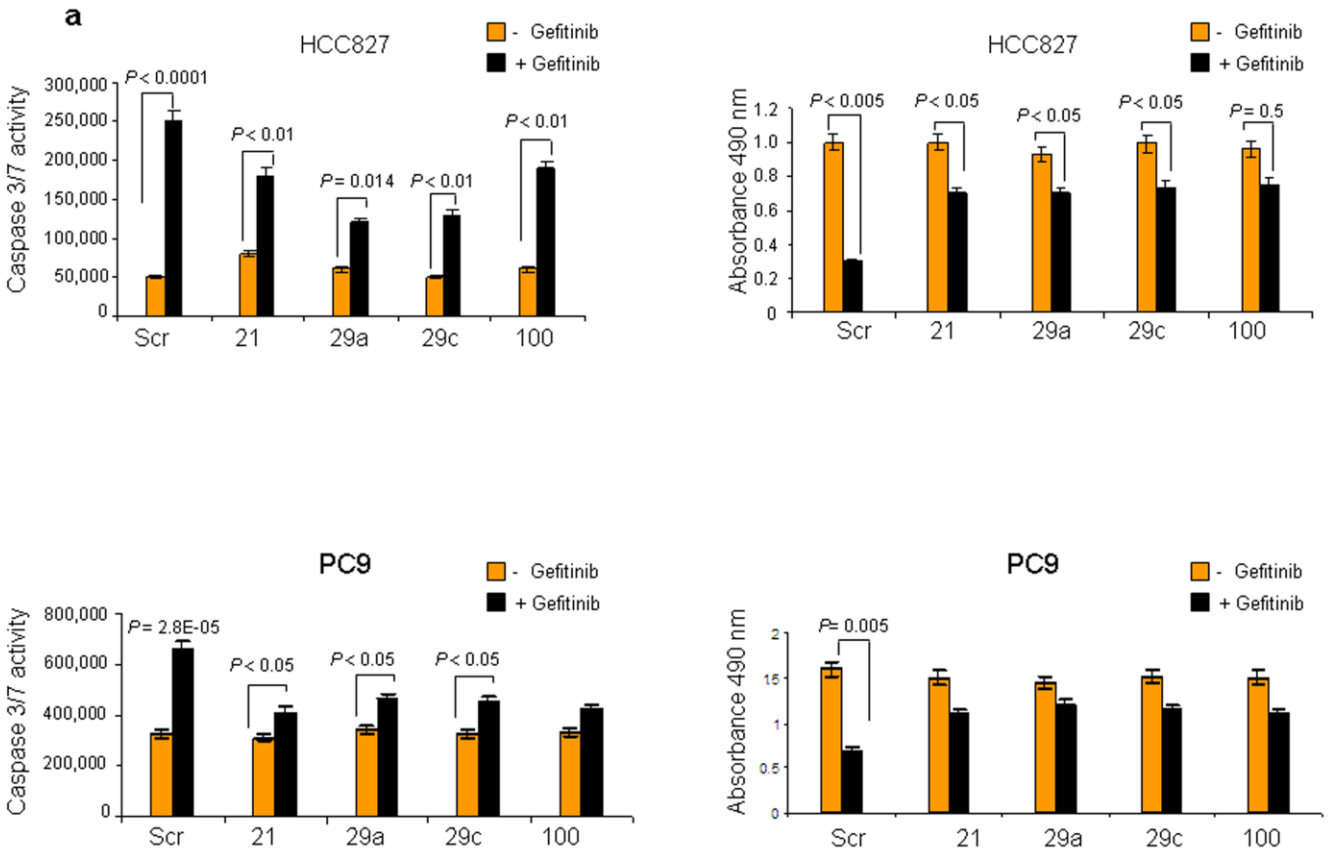

Supplementary Figure 10. MiR-21, 29a/c, 100 are involved in gefitinib-induced apoptosis. (**a**) Enforced expression of miR-21, 29a/c, 100 increases cell viability and reduces caspase 3/7 activity in HCC827 and PC9 cells exposed to 10μM gefitinib for 24h. One representative of three independent experiments is shown. Relative values are shown as mean and ± s.d. Two tailed student's t test was used to determine *P* values.

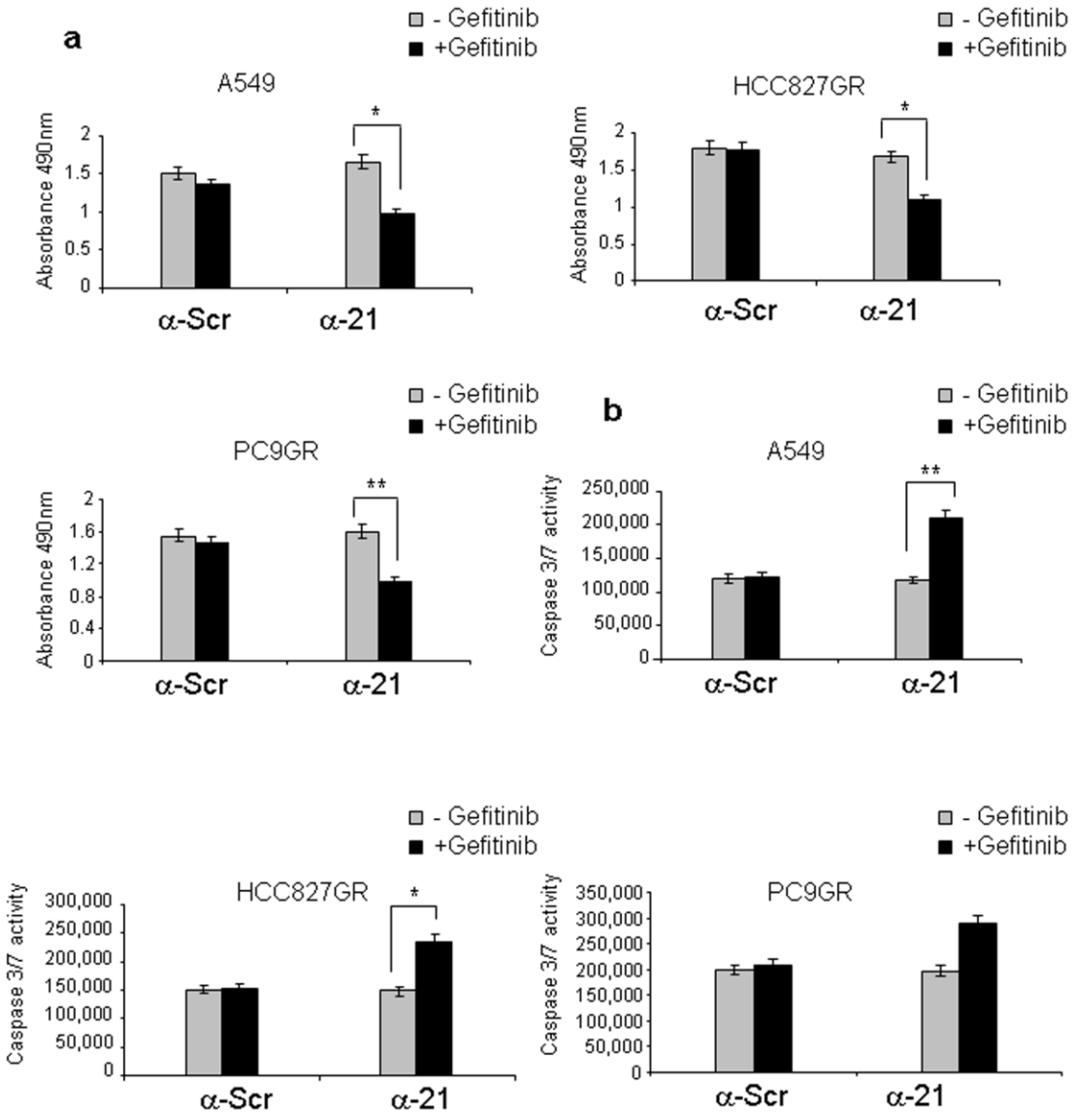
a
- Gefitinib
+Gefitinib
A549
Absorbance 490nm
2
1.5
1
0.5
0
*
α-Scr
α-21
- Gefitinib
+Gefitinib
HCC827GR
Absorbance 490nm
2
1.5
1
0.5
0
*
α-Scr
α-21
- Gefitinib
+Gefitinib
PC9GR
Absorbance 490nm
2
1.6
1.2
0.8
0.4
0
**
α-Scr
α-21
b
- Gefitinib
+Gefitinib
A549
Caspase 3/7 activity
250,000
200,000
15,0000
100,000
50,000
0
**
α-Scr
α-21
- Gefitinib
+Gefitinib
HCC827GR
Caspase 3/7 activity
300,000
250,000
200,000
150,000
100,000
50,000
0
*
α-Scr
α-21
- Gefitinib
+Gefitinib
PC9GR
Caspase 3/7 activity
350,000
300,000
250,000
200,000
150,000
100,000
50,000
0
α-Scr
α-21

Supplementary Figure 11. MiR-21 knockdown increases gefitinib sensitivity. (**a**) MiR-21 silencing by anti-miR oligonucleotides in A549, HCC827GR and PC9GR cells decreases cell viability as assessed by MTS assay and (**b**) increases cell death, by caspase 3/7 assay, after gefitinib treatment (10μM) for 24h. Error bars depict s.d. Results from at least three independent experiments are reported. **P*< 0.05, ***P*< 0.001 by two tailed student *t* test.

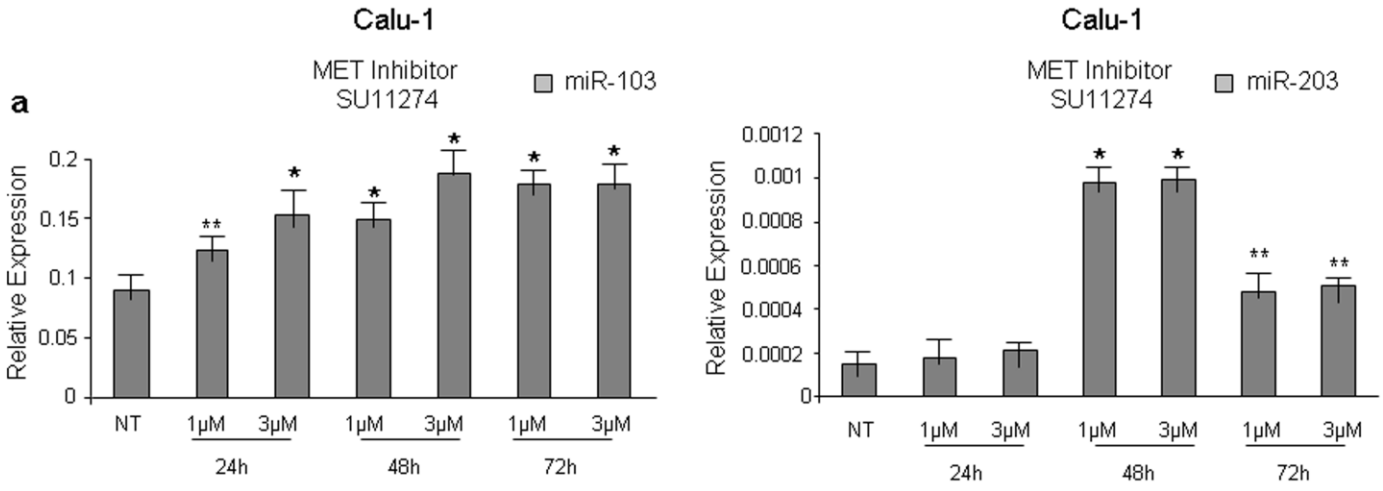

Supplementary Figure 12. MET inhibitor SU11274 induces miR-103 and 203 upregulation. (**a**) Calu-1 cells were exposed to different SU11274 concentrations (1 and 3μM) for 24, 48 and 72h. MiR-103 and -203 expression levels were assessed by qRT-PCR as described in the Supplementary Methods. Results are representative of at least, three independent experiments. Error bars depict ± s.d. *P<0.001, ** P<0.05.

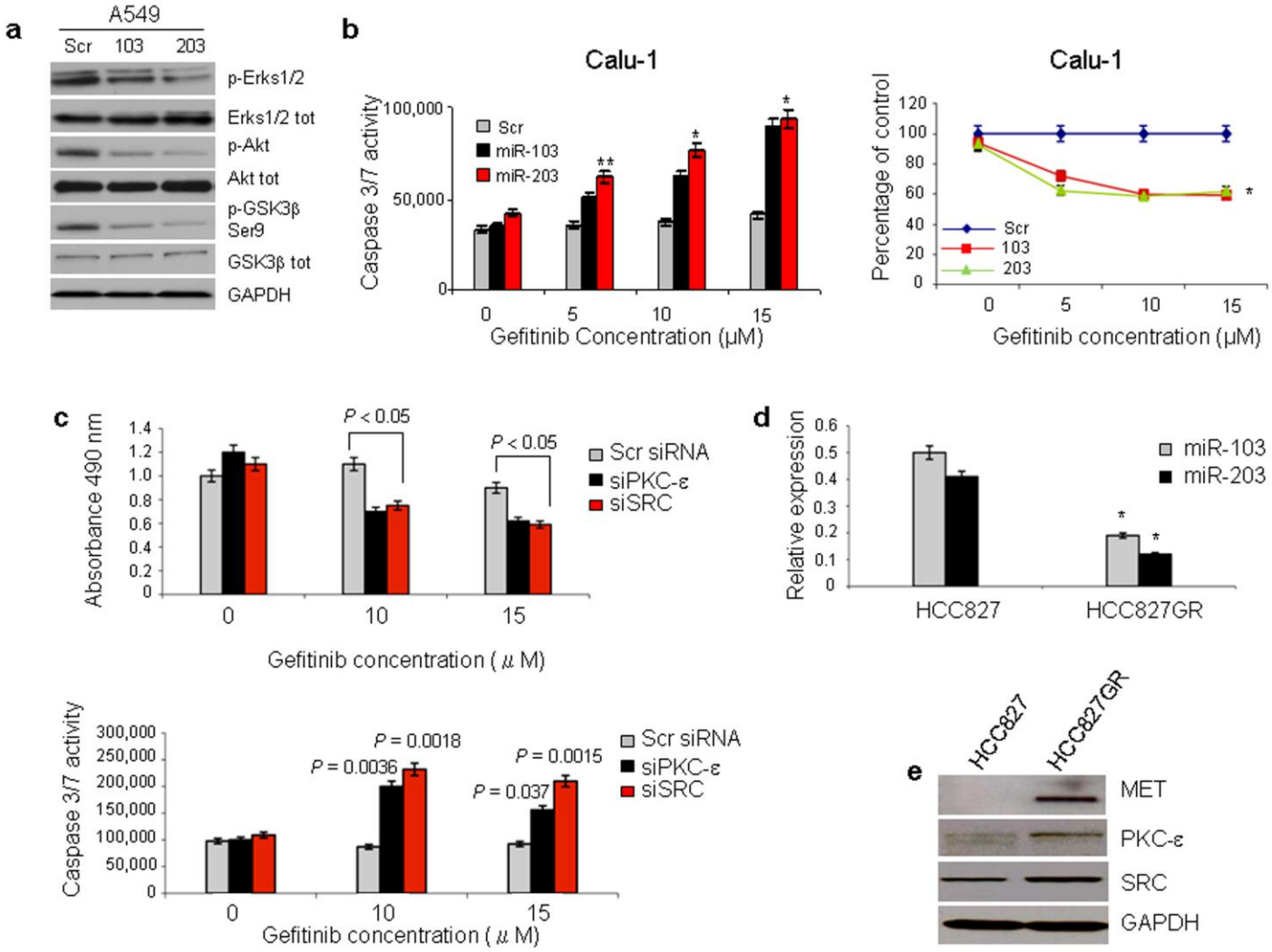

Supplementary Figure 13. PKC-ε and SRC knockdown induces gefitinib sensitivity. (**a**) MiR-103,-203 enforced expression in A549 cells inhibits the AKT/ERKs pathways. β-

actin levels were used as loading control. One representative of three independent experiments is shown. (**b**) MiR-103, -203 overexpression in Calu-1 cells induces gefitinib sensitivity as assessed by caspase 3/7 and MTT assays. Results are representative of at least four independent experiments. (**c**) Viability and caspase 3/7 assays in Calu-1 cells after PKC-ε and SRC knockdown followed by gefitinib treatment (10μM, 15μM) for 24h. **(d)** qRT-PCR showing miR-103 and -203 decreased expression in HCC827GR cells, with MET amplification, compared to the parental HCC827 cells. (**e**) Western blot showing increased expression of PKC-ε and SRC in HCC827GR with MET amplification, compared to the parental HCC827 gefitinib-sensitive cells. Experiments were performed three times in triplicate. Error bars represent standard deviation. *P* values were obtained by Student's *t* test. **P*<0.005.

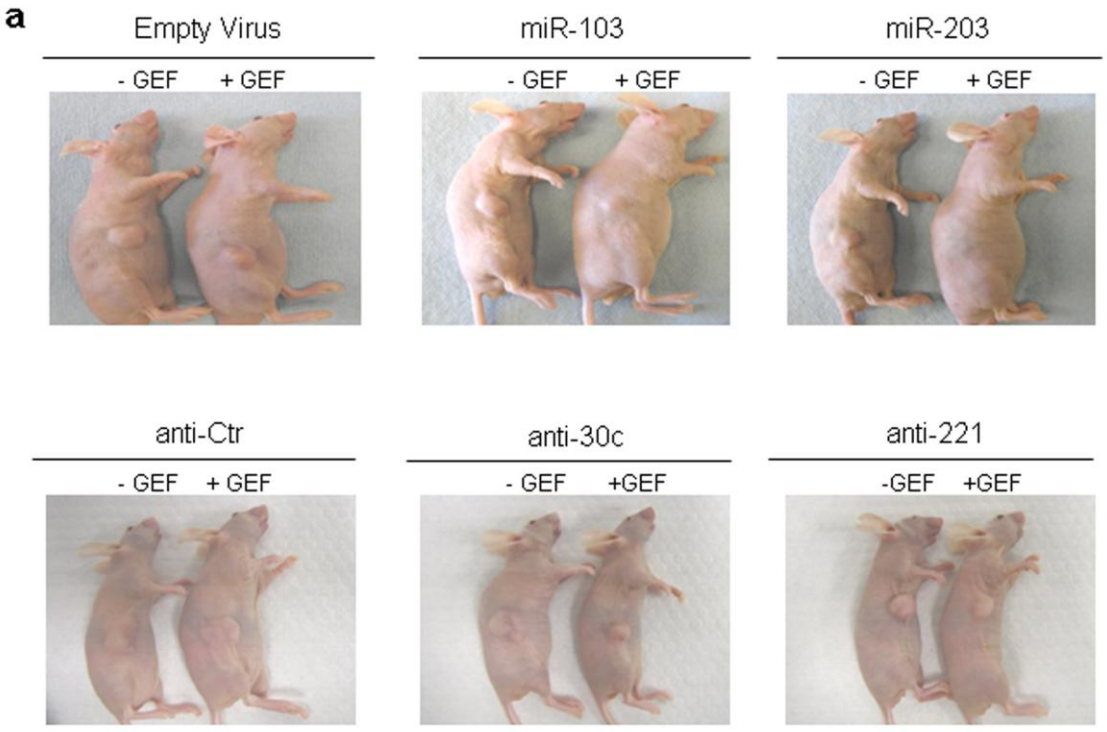
a
Empty Virus
- GEF + GEF
miR-103
- GEF + GEF
miR-203
- GEF + GEF
anti-Ctr
- GEF + GEF
anti-30c
- GEF +GEF
anti-221
-GEF +GEF

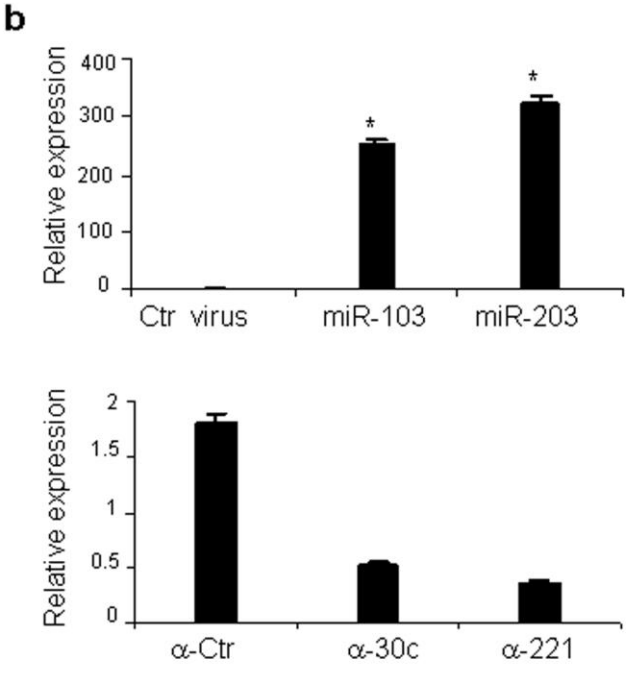
b
Relative expression
400
300
200
100
0
*
*
Ctr virus
miR-103
miR-203
Relative expression
2
1.5
1
0.5
0
α-Ctr
α-30c
α-221

Supplementary Figure 14. MiR-103, 203, 221, 30c effects *in vivo*. (**a**) Comparison of tumor engraftments in nude mice injected with A549 cells stable infected with Empty virus, miR-103, miR-203 and with anti-Ctr, anti-221, anti-30c. 35 days from the injection and after treatment with vehicle (0.1% tween 80) or gefitinib (200mg/kg) mice were sacrificed. The images show one mouse from among five of each category. (**b**) qRT-PCR showing miR-103, -203 upregulation and miR-30c, 221 downregulation in tumor xenografts. Data are presented as ± s.d. **P* <0.001.

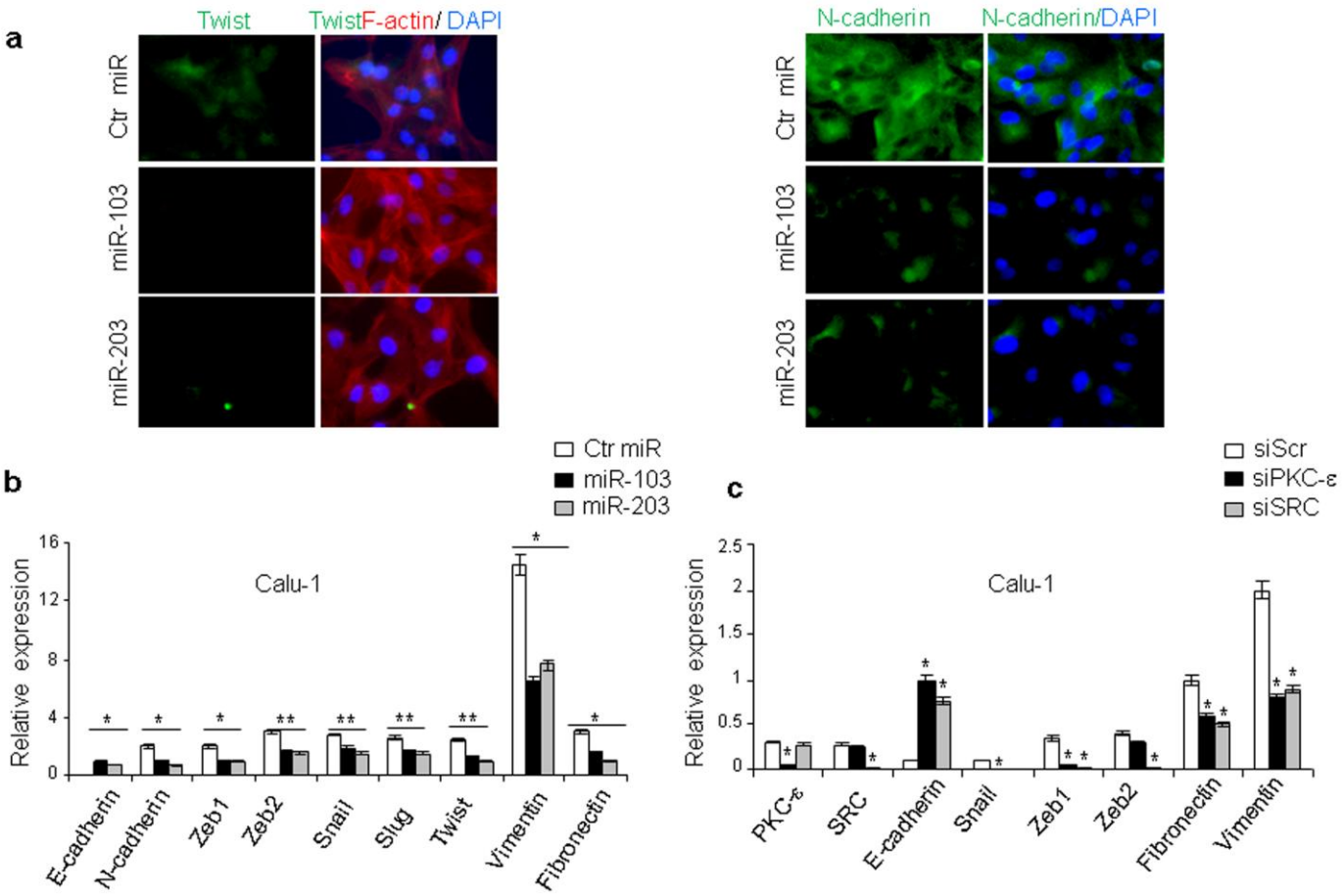

Supplementary Figure 15. MiR-103 and 203 overexpression induces MET. (**a**) Immunofluorescence showing Twist and N-cadherin downregulation after miR-103 and -203 enforced expression. (**b-c**) qRT-PCRs after miR-103 and -203 enforced expression and *PKC-ε* and *SRC* silencing in Calu-1 cells. MiR-103, -203 overexpression and *PKC-ε*, *SRC* knockdown induces a decrease in mesenchymal markers and an increase in E-cadherin mRNAs expression levels. Error bars depict s.d. Results from at least three independent experiments are reported. **P*< 0.001, ***P*< 0.05.

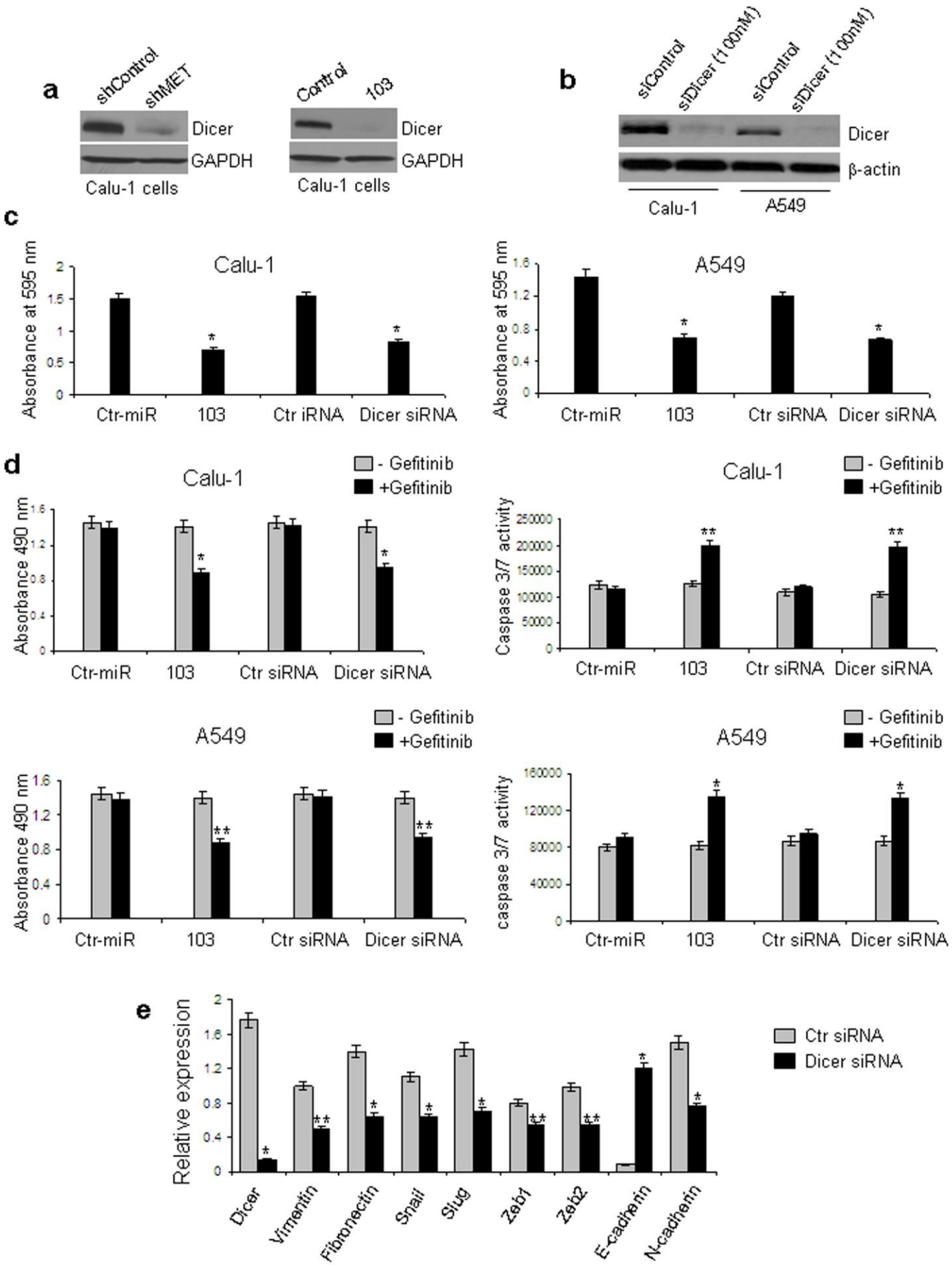
a
shControl
shMET
Dicer
GAPDH
Calu-1 cells
Control
103
Dicer
GAPDH
Calu-1 cells
b
siControl
siDicer (100nM)
siControl
siDicer (100nM)
Dicer
β-actin
Calu-1
A549
c
Calu-1
Absorbance at 595 nm
Ctr-miR
103
Ctr iRNA
Dicer siRNA
A549
Absorbance at 595 nm
Ctr-miR
103
Ctr siRNA
Dicer siRNA
d
Calu-1
- Gefitinib
+Gefitinib
Absorbance 490 nm
Ctr-miR
103
Ctr siRNA
Dicer siRNA
Calu-1
- Gefitinib
+Gefitinib
Caspase 3/7 activity
Ctr-miR
103
Ctr siRNA
Dicer siRNA
A549
- Gefitinib
+Gefitinib
Absorbance 490 nm
Ctr-miR
103
Ctr siRNA
Dicer siRNA
A549
- Gefitinib
+Gefitinib
caspase 3/7 activity
Ctr-miR
103
Ctr siRNA
Dicer siRNA
e
Relative expression
Ctr siRNA
Dicer siRNA
Dicer
Vimentin
Fibronectin
Snail
Slug
Zeb1
Zeb2
E-cadherin
N-cadherin

Supplementary Figure 16. Dicer silencing promotes gefitinib sensitivity and MET in NSCLC. (**a**) Dicer down-regulation after MET stable knockdown and after miR-103 enforced expression in Calu-1 cells. (**b**) Dicer downregulation after transfection of Calu-1 and A549 cells with 100 nM of Dicer siRNA**.** (**c**) Dicer knockdown reduces cell migration in Calu-1 and A549 cells. Graphs show the absolute number of cells migrating through the transwell quantified by measuring the absorbance at 595 nm. (**d**) MTS and caspase 3/7 assays (**c**) showing how Dicer silencing increases sensitivity to gefitinib-induced apoptosis. Results are representative of at least, three independent experiments. (**e**) qRT-PCR showing that Dicer depletion influences mesenchymal-epithelial transition (MET) by regulating the expression of mesenchymal and epithelial markers. Error bars depict ± s.d. of four independent experiments in **c** and **d**. * $P<0.005$, ** $P<0.05$.

Supplementary Table 1

Lung tumors (TMAs) clinical data.

	Age	Gender	Grade	Stage	Metastases	Tumor Hystotype
1	65	M	2	IIIa	yes	Squamous cell carcinoma
2	65	M	1	IIIa	no	Squamous cell carcinoma
3	53	M	2	II	yes	Squamous cell carcinoma with necrosis
4	46	M	1	IIIa	no	Squamous cell carcinoma
5	68	M	1	II	yes	Squamous cell carcinoma
6	43	F	1	II	yes	Squamous cell carcinoma
7	57	M	2	IIIa	yes	Squamous cell carcinoma
8	57	M	-	I	no	Squamous cell carcinoma (sparse)
9	68	F	2	II	yes	Squamous cell carcinoma with necrosis
10	69	M	2	I	no	Squamous cell carcinoma with necrosis
11	69	M	1	IIIa	yes	Squamous cell carcinoma
12	66	M	1	I	no	Squamous cell carcinoma

13	47	M	2	I	no	Squamous cell carcinoma
14	50	F	2	I	no	Squamous cell carcinoma
15	44	M	2	II	yes	Squamous cell carcinoma
16	50	M	2	IIIa	yes	Squamous cell carcinoma
17	63	M	1	IIIa	yes	Squamous cell carcinoma
18	46	M	1	I	no	Squamous cell carcinoma
19	43	M	2	I	no	Squamous cell carcinoma
20	68	M	2	IIIa	yes	Squamous cell carcinoma
21	65	M	2	I	no	Squamous cell carcinoma
22	51	M	2	I	no	Squamous cell carcinoma
23	55	M	2	I	no	Squamous cell carcinoma
24	41	M	-	IIIa	yes	Squamous cell carcinoma (chronic inflammation of fibrous tissue and blood vessel)
25	66	M	2	I	no	Squamous cell carcinoma
26	61	M	2	I	no	Squamous cell carcinoma
27	63	M	2	IIIa	yes	Squamous cell carcinoma
28	63	M	2	I	no	Squamous cell carcinoma
29	51	M	2	IIIa	no	Squamous cell carcinoma
30	61	M	3	IIIa	yes	Squamous cell carcinoma
31	66	M	2	II	yes	Squamous cell carcinoma
32	66	M	2	IIIa	yes	Squamous cell carcinoma
33	60	F	2	II	yes	Squamous cell carcinoma
34	56	M	3	II	yes	Squamous cell carcinoma
35	51	F	-	IIIa	yes	Squamous cell carcinoma (interstitial pneumonia)
36	46	M	2	I	no	Squamous cell carcinoma
37	60	M	3	I	no	Squamous cell carcinoma
38	44	M	3	I	no	Squamous cell carcinoma
39	65	M	2	I	no	Squamous cell carcinoma with necrosis
40	71	M	2	I	no	Squamous cell carcinoma
41	61	M	2	I	no	Squamous cell carcinoma
42	52	M	-	I	no	Adenosquamous carcinoma
43	43	F	-	I	no	Adenosquamous carcinoma
44	50	M	1	II	yes	Mucinous adenocarcinoma
45	70	M	1	I	no	Papillary adenocarcinoma
46	42	M	1	I	no	Mucinoius adenocarcinoma
47	48	F	1	I	no	Mucinoius adenocarcinoma
48	64	F	1	II	yes	Mucinoius adenocarcinoma
49	62	F	3	II	yes	Adenocarcinoma
50	44	F	1	IIIa	yes	Adenocarcinoma
51	43	F	2	IIIa	yes	Adenocarcinoma with necrosis
52	63	M	2	IIIa	yes	Adenocarcinoma

53	51	M	2	IIIa	yes	Adenocarcinoma
54	63	F	2	II	yes	Adenocarcinoma
55	50	M	2	IIIa	yes	Adenocarcinoma
56	44	F	2	II	yes	Adenocarcinoma
57	56	M	2	IIIa	no	Adenocarcinoma
58	71	F	2	II	yes	Adenocarcinoma
59	56	F	1	II	yes	Adenocarcinoma
60	50	F	1	I	no	Papillary adenocarcinoma
61	56	F	2	I	no	Adenocarcinoma
62	67	M	2	II	yes	Adenocarcinoma (sparse)
63	59	M	2	IIIa	yes	Adenocarcinoma
64	61	M	2	I	no	Adenocarcinoma
65	50	M	2	I	no	Adenocarcinoma
66	61	F	2	II	yes	Adenocarcinoma
67	60	F	2	I	no	Adenocarcinoma
68	66	M	2	II	yes	Adenocarcinoma
69	68	F	2	IIIa	yes	Adenocarcinoma with necrosis
70	55	F	2	I	no	Adenocarcinoma
71	50	F	2	IIIa	yes	Adenocarcinoma
72	57	M	2	II	yes	Adenocarcinoma
73	50	M	2--3	II	yes	Adenocarcinoma
74	68	M	2--3	IV	yes	Adenocarcinoma
75	60	M	2--3	II	yes	Adenocarcinoma
76	51	F	2--3	I	no	Adenocarcinoma
77	68	M	2	II	yes	Adenocarcinoma
78	64	F	2--3	I	no	Adenocarcinoma
79	59	F	-	IIIa	yes	Adenocarcinoma (sparse)
80	53	M	3	I	no	Adenocarcinoma
81	57	F	2	I	no	Adenocarcinoma
82	48	F	2--3	I	no	Adenocarcinoma
83	60	M	3	IIIa	yes	Adenocarcinoma
84	54	M	3	I	no	Adenocarcinoma
85	76	M	3	II	yes	Adenocarcinoma
86	67	M	3	IIIa	no	Adenocarcinoma
87	35	F	3	I	no	Adenocarcinoma
88	68	F	3	IIIa	yes	Adenocarcinoma
89	57	M	-	I	no	Adenocarcinoma (lung tissue)
90	42	M	3	IIIa	yes	Adenocarcinoma
91	59	M	2	II	yes	Adenocarcinoma
92	51	F	-	I	no	Bronchioloalveolar carcinoma
93	72	M	-	I	no	Bronchioloalveolar carcinoma
94	60	M	-	II	yes	Bronchioloalveolar carcinoma (carcinoma sparse with necrosis)
95	53	M	-	II	no	Bronchioloalveolar carcinoma

96	53	M	-	IIIb	no	Large cell carcinoma
97	54	F	-	II	yes	Large cell carcinoma
98	54	M	-	I	no	Large cell carcinoma
99	65	M	-	I	no	Large cell carcinoma
100	51	F	-	I	yes	Small cell undifferentiated carcinoma
101	39	M	-	II	yes	Small cell undifferentiated carcinoma
102	42	F	-	IIIb	yes	Small cell undifferentiated carcinoma
103	73	M	-	IIIa	yes	Small cell undifferentiated carcinoma
104	32	F	-	II	yes	Small cell undifferentiated carcinoma
105	61	M	-	I	no	Small cell undifferentiated carcinoma
106	60	M	-	I	no	Atypical carcinoid
107	57	M	-	I	no	Atypical carcinoid
108	36	F	-	I	no	Atypical carcinoid
109	49	M	-	IIIb	yes	Atypical carcinoid
110	43	M	-	I	yes	Carcinoid

Supplementary Table 2

Lung tumor specimens' clinical data

sclc=small cell lung cancer; nsclc=non-small cell lung cancer

	Age	Race	Gender	Tumor Size (gr.)	Metastatic	Tumor Hystotype
1	76	white	F	0.4	no	Adenocarcinoma
2	70	white	M	0.45	yes (adrenal)	adenocarcinoma
3	61	white	M	0.4	no	sclc
4	75	white	F	0.3	no	adenocarcinoma
5	55	white	M	0.3	no	adenocarcinoma
6	60	white	F	0.4	no	squamous cell carcinoma
7	72	white	F	0.4	no	squamous cell carcinom
8	51	white	F	0.4	yes (thyroid)	adenocarcinoma
9	69	white	M	0.4	no	sclc
10	66	white	F	0.4	yes (lymphonode)	squamous cell carcinoma
11	59	white	M	0.4	no	adenocarcinoma
12	79	white	M	1	yes (lymphonode)	adenocarcinoma
13	72	black	F	0.41	no	squamous cell carcinoma
14	65	white	F	0.45	yes (liver)	adenocarcinoma
15	73	white	M	0.4	yes (colon)	adenocarcinoma
16	69	white	M	0.51	no	adenocarcinoma
17	55	white	F	0.48	yes (lymphonode)	adenocarcinoma
18	77	white	M	0.4	yes (brain)	nsclc
19	58	black	M	0.4	no	adenocarcinoma
20	68	white	M	0.4	no	adenocarcinoma
21	47	white	M	0.4	yes (lymphonode)	adenocarcinoma
22	58	white	F	0.4	no	nsclc
23	70	white	M	0.45	no	squamous cell carcinoma
24	50	white	F	0.4	no	adenocarcinoma
25	70	white	M	0.42	no	nsclc
26	50	black	M	0.4	no	squamous cell carcinoma
27	73	white	M	0.4	yes (lymphonode)	nsclc
28	61	black	M	0.4	yes (brain)	squamous cell carcinoma
29	67	white	F	0.4	no	typical carcinoid
30	68	white	F	0.55	yes (brain)	adenocarcinoma
31	74	white	M	0.5	no	adenocarcinoma
32	76	white	M	0.4	no	adenocarcinoma
33	61	white	F	0.4	yes (lymphonode)	adenocarcinoma
34	64	white	F	0.5	yes (lymphonode)	nsclc
35	79	white	F	0.43	no	adenocarcinoma
36	74	white	F	0.46	yes (liver)	nsclc
37	42	black	M	0.4	no	nsclc
38	71	white	F	0.45	no	squamous cell carcinoma
39	56	white	F	0.4	yes (brain)	nsclc
40	80	white	M	0.4	yes (liver)	adenocarcinoma